

Review

# Noble-Metal-Based Catalytic Oxidation Technology Trends for Volatile Organic Compound (VOC) Removal

Hyo-Sik Kim <sup>1</sup>, Hyun-Ji Kim <sup>1</sup>, Ji-Hyeon Kim <sup>1</sup>, Jin-Ho Kim <sup>1</sup>, Suk-Hwan Kang <sup>1</sup>, Jae-Hong Ryu <sup>1,\*</sup>, No-Kuk Park <sup>2</sup>, Dae-Sik Yun <sup>3</sup> and Jong-Wook Bae <sup>4,\*</sup>

<sup>1</sup> Plant Engineering Center, Institute for Advanced Engineering (IAE), Yongin-si 17180, Korea; hyosgogo@iae.re.kr (H.-S.K.); hj.kim@iae.re.kr (H.-J.K.); kimjyun@iae.re.kr (J.-H.K.); jinho@iae.re.kr (J.-H.K.); shkang@iae.re.kr (S.-H.K.)

<sup>2</sup> School of Chemical Engineering, Yeungnam University, Gyeongsan 38541, Korea; nokukpark@ynu.ac.kr

<sup>3</sup> ChangSung Engineering Co., Ltd., Buk-gu, Gwangju 61003, Korea; daesik\_yun@yahoo.com

<sup>4</sup> School of Chemical Engineering, Sungkyunkwan University (SKKU), Suwon-si 16419, Korea

\* Correspondence: jhryu@iae.re.kr (J.-H.R.); finejw@skku.edu (J.-W.B.); Tel.: +82-31-330-7882 (J.-H.R.); +82-31-290-7347 (J.-W.B.); Fax: +82-31-330-7333 (J.-H.R.); +82-31-290-7272 (J.-W.B.)

**Abstract:** Volatile organic compounds (VOCs) are toxic and are considered the most important sources for the formation of photochemical smog, secondary organic aerosols (SOAs), and ozone. These can also greatly affect the environment and human health. For this reason, VOCs are removed by applying various technologies or reused after recovery. Catalytic oxidation for VOCs removal is widely applied in the industry and is regarded as an efficient and economical method compared to other VOCs removal technologies. Currently, a large amount of VOCs are generated in industries with solvent-based processes, and the ratio of aromatic compounds is high. This paper covers recent catalytic developments in VOC combustion over noble-metal-based catalysts. In addition, this report introduces recent trends in the development of the catalytic mechanisms of VOC combustion and the deactivation of catalysts, such as coke formation, poisoning, sintering, and catalyst regeneration. Since VOC oxidation by noble metal catalysts depends on the support of and mixing catalysts, an appropriate catalyst should be used according to reaction characteristics. Moreover, noble metal catalysts are used together with non-noble metals and play a role in the activity of other catalysts. Therefore, further elucidation of their function and catalytic mechanism in VOC removal is required.

**Keywords:** VOC removal; catalytic oxidation; noble metal catalyst; catalyst deactivation; catalyst regeneration



**Citation:** Kim, H.-S.; Kim, H.-J.; Kim, J.-H.; Kim, J.-H.; Kang, S.-H.; Ryu, J.-H.; Park, N.-K.; Yun, D.-S.; Bae, J.-W. Noble-Metal-Based Catalytic Oxidation Technology Trends for Volatile Organic Compound (VOC) Removal. *Catalysts* **2022**, *12*, 63. <https://doi.org/10.3390/catal12010063>

Academic Editor: Fan Lin

Received: 20 December 2021

Accepted: 2 January 2022

Published: 7 January 2022

**Publisher's Note:** MDPI stays neutral with regard to jurisdictional claims in published maps and institutional affiliations.



**Copyright:** © 2022 by the authors. Licensee MDPI, Basel, Switzerland. This article is an open access article distributed under the terms and conditions of the Creative Commons Attribution (CC BY) license (<https://creativecommons.org/licenses/by/4.0/>).

## 1. Introduction

Volatile organic compounds (VOCs) are liquid or gaseous organic compounds that easily evaporate into the atmosphere due to their low boiling point. All carbon compounds, except for the negligible substances designated by the EPA (United States Environmental Protection Agency, Washington, DC, USA), are included in VOCs. The WHO (World Health Organization, Geneva, Switzerland) classifies VOCs according to their ease of release based on their boiling point measured at 101.3 kPa: VVOC (very volatile organic compounds,  $B_T$  (Boring temperature): ~0 to 50~100 °C), VOC (volatile organic compounds,  $B_T$ : 50~100 to 240~260 °C), and SVOC (semi-volatile organic compounds,  $B_T$ : 240~260 to 380~400 °C) [1].

Currently, the main sources of VOCs emission sources include gasoline/diesel vehicles, construction equipment, electric utilities, petrochemicals, and odor handling process, as well as the paint, solvent, adhesive, and synthetic resin manufacturing industries [2]. According to Li et al., China, had the highest contribution to global VOC emissions, as of 2017. They also reported that 33% of the total VOCs are aromatic compounds with the highest content in the order of toluene > xylene > ethylene > acetylene > benzene > others [3]. Brown et al. examined the main sources of VOCs in LA and observed that approximately 50% of all

VOCs originated from processes that use solvents [4]. Similarly, in Korea, approximately 53% of total VOCs are emitted from the paint, ink, and print manufacturing facilities [5].

VOCs emissions from various sources typically include BTEX (benzene, ethylbenzene, toluene, xylene), alcohols, esters, and organic solvents. VOCs, such as BTEX and ethylene, are precursors that generate ozone and photochemical smog through photochemical reactions with nitrogen oxides (NO<sub>x</sub>) in the atmosphere, thereby contributing to global warming. VOCs are also known as secondary fine dust precursors [6]. The effective removal of VOCs may reduce the emission of fine dust generating materials, which is a significant focus of research at present [7]. Additionally, based on the risk of VOCs to humans, according to the carcinogenic substance classification system by the International Agency for Research on Cancer (IARC), benzene, 1,3-butadiene, formaldehyde, trichloroethylene, among others, are carcinogenic to humans (group 1). Furthermore, tetrachloroethylene is classified as a putative substance and is probably carcinogenic to humans (group 2A).

Technologies for VOC emission reduction can be broadly divided into two types. The first one is a method of degrading VOCs using chemical conversion, such as oxidation or decomposition, and the second one is a method of adsorbing or recovering VOCs without chemical conversion and reusing it. Examples of methods using chemical conversion include oxidation using fuel or decomposition using UV or microorganisms. This method has a disadvantage in that VOCs cannot be recovered; this is a major drawback especially when the target VOCs are expensive. Examples of separation and recovery technologies include adsorption and film separation, as well as condensation using cooling. In this case, VOCs are mixed with different components, and this method has a disadvantage in that the total removal rate is reduced based on the selective adsorption capacity of adsorbents [8–10].

Catalysts used for the oxidation of VOCs include noble metals, non-noble metals, and perovskite. Noble-metal-based catalysts are widely used owing to their effectiveness for low-temperature VOC oxidation and high BTEX oxidation efficiency. Although research on non-noble-metal-based catalysts has been conducted, their application is limited due to several issues, such as difficult disposal, high toxicity, and low activity. Additionally, since many studies use a mixture of non-noble metals with a noble metal catalyst to increase VOC oxidation efficiency, it is essential to examine the characteristics of the noble metal catalyst in detail.

This review investigates a combustion catalyst that converts VOCs, which are hydrocarbon compounds, into carbon dioxide and water, and discharges them through a combustion reaction during chemical conversion. In particular, the BTEX-based combustion catalyst has been described, which is relatively difficult to oxidize due to its large and stable molecular structure that includes a benzene ring. Further, the characteristics of noble-metal-based combustion catalyst technology are investigated.

## 2. Catalytic Combustion Mechanism of Noble Metal Catalysts

### 2.1. Kinetic Analysis

To explain the VOC oxidation mechanism, many researchers have proposed a three-mechanism model: (a) Langmuir–Hinshellwood (L–H) model, (b) Eley–Rideal (E–R) model, and (c) Mars–Van Krevelen (MVK) model (two-stage redox) with the Pd-based catalysts (Figure 1 and Table 1). The (a) mechanism model emphasizes the interaction between two molecules adsorbed at the active sites of the solid metal surface, while the surface reaction between adsorbed reactants and gaseous molecules was included in the (b) mechanism model. The (c) mechanism model assumes that the oxygen surface concentration of the catalyst is constant, and the reaction occurs through the interaction of the reactant molecule and the oxidized sites of the catalyst surface [11–22].

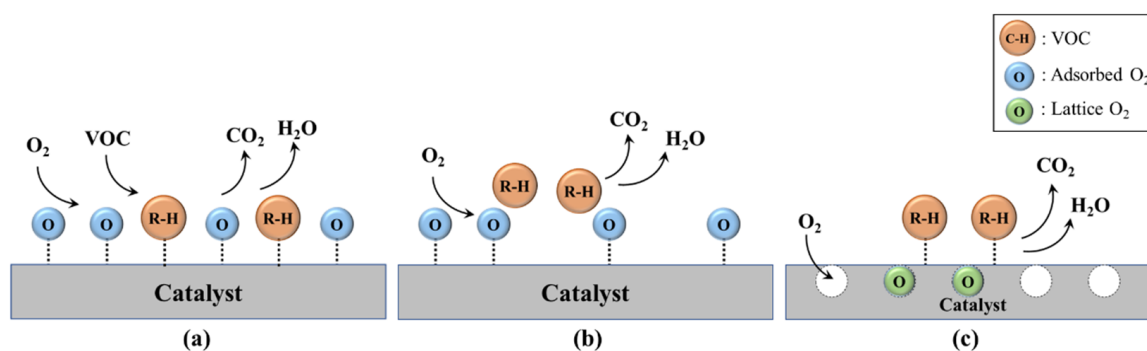


**Figure 1.** Kinetic models of catalytic VOC oxidation: (a) L–H model, (b) E–R model, and (c) MVK model.

**Table 1.** Kinetic models of catalytic VOC oxidation.

Catalyst	Support	VOCs	Kinetic Model	Ref.
Ag	Mn <sub>2</sub> O <sub>3</sub>	Toluene	MVK	[11]
Au	Meso-Co <sub>3</sub> O <sub>4</sub>	Benzene	MVK	[12]
Pd	CeO <sub>2</sub>	Toluene	MVK	[13]
Pd	ZSM-5	Benzene	MVK	[14]
Pd–Ce	γ-Al <sub>2</sub> O <sub>3</sub>	Toluene	MVK	[15]
Pd	activated-C	Toluene	L–H	[16]
Pd	Al <sub>2</sub> O <sub>3</sub>	TCE	E–R	[17]
Pt	γ-Al <sub>2</sub> O <sub>3</sub>	Toluene	MVK	[18]
Pt	γ-Al <sub>2</sub> O <sub>3</sub>	Benzene	MVK	[19]
Pt	γ-Al <sub>2</sub> O <sub>3</sub>	Cyclooctane	E–R	[20]
Pt	Al <sub>2</sub> O <sub>3</sub>	Xylene	L–H	[20]
Pt	CeO <sub>2</sub>	Toluene	L–H	[21]

As shown in Table 1, an MVK kinetic model is generally used to explain the oxidation reaction of VOCs on Pd catalysts. Unlike general Pd-based catalysts, the L–H model applies to the oxidation of toluene (C<sub>7</sub>H<sub>8</sub>) over Pd/C catalysts with activated carbon as a support [16]. Additionally, the E–R model was applied to the catalytic oxidation of trichloroethylene (TCE) using Pd/Al<sub>2</sub>O<sub>3</sub> catalysts [15]. Overall, it has been reported that the effect of each mechanism is determined by the catalyst composition and VOC component. Alejo et al. investigated the mechanism of the toluene oxidation reaction through an intermediate analysis of the Pd/CeO<sub>2</sub> catalyst. The role of the Pd catalyst in the MVK mechanism was also investigated, and it was found to promote lattice oxygen generation [13]. Recently, Manta et al. investigated cycloalkane (cyclooctane) oxidation on Pt/γ-alumina using an E–R kinetic model, whereas catalytic *o*-xylene combustion over Pt/γ-alumina was described by the L–H mechanism model [20].

The kinetic model of the catalytic VOC (ethyl acetate and toluene) combustion over Au/MeO<sub>x</sub> (Me = Mg, Fe, Ni, Cu, Y, and La) [23] and Pd/ZSM-5 [14] was a good fit for the MVK model. Shengsheng et al. [21] evaluated the activity of the toluene oxidation reaction by varying the oxygen vacancy concentration while changing the surface exposure of the Pt/CeO<sub>2</sub> catalyst; the main reaction was achieved through the L–H model. The catalytic oxidation of propene over Au–MeO<sub>x</sub>/Al<sub>2</sub>O<sub>3</sub> (Me = Mn, Fe, Co, and Ce) [24] and methyl-ethyl-ketone (MEK) over Pd–Mn/Al<sub>2</sub>O<sub>3</sub> [25] obeyed the MVK model. In addition, the MVK model applied to the catalytic oxidation reaction of oxygenated hydrocarbons (methanol) on Pd/Y [26] and alkanes (isobutane) on Au–MeO<sub>x</sub>/CeO<sub>2</sub> (Me = Mn, Fe, Co, and Ni) [27]. Thus, most researchers have analyzed the catalytic oxidation of noble metal catalysts using the MVK model.

## 2.2. Mechanism Studies

To remove VOCs, the mechanism of catalytic VOC combustion over noble metal catalysts was classified into hydrocarbons, oxygen-containing hydrocarbons, and chlorine-containing hydrocarbons, as presented in the following sections.

### 2.2.1. Hydrocarbons

The mechanism of catalytic propane combustion over a Pt catalyst supported on various zeolites (e.g., ZSM-5, Beta, HY, and KL) was reported by Garetto et al. [28]. The rate-determining step was suggested to be dissociative chemisorption of propane on Pt through interaction with surrounding adsorbed oxygen atoms after the weakest C–H bond was broken. Consequently, propane adsorption occurs, and propane molecules are activated at the surface-active sites present in the metal oxide through a parallel oxidation pathway and react with excess oxygen from the metal active sites.

Yang et al. investigated catalytic ethylene oxidation using Ag catalysts supported on zeolites (e.g., ZSM-5, Beta, Y, and MOR) [29]. The reaction mechanism by which ethylene is catalytically oxidized occurs in different stages. First, ethylene is adsorbed and activated at the Brønsted acid sites present in Ag-metal-supported zeolite catalysts. The activated ethylene species are attacked by reactive oxygen species (ROS), resulting in the formation of formaldehyde by breaking the C–C bond of ethylene species. Subsequently, formaldehyde produced on the catalyst surface is continuously oxidized to CO<sub>2</sub> and H<sub>2</sub>O.

A catalytic study on the mechanism of propene combustion was conducted by Weng et al. [30]. To elucidate the mechanism, Pt metal was supported on alumina, and BaO was used as an additive. Propene is adsorbed and activated at the catalytically active site, converted to carboxylate, and formed acrylate. In this case, when BaO was used as an additive in the catalytic reaction, improved reactivity was obtained while inducing the generation of more reactive enolic species. Consequently, ROS increases on the metal surface (Pt-Ba) of the catalyst, which also increases the CO oxidation rate.

### 2.2.2. Oxygen-Containing Hydrocarbons

The catalytic combustion mechanism of 2-propanol was proposed by Liu and Yang using an Au-based catalyst [31]. Similar to other mechanisms, the first step in the mechanism of 2-propanol oxidation over the Au/CeO<sub>2</sub> catalyst is the adsorption of 2-propanol onto the catalyst. Subsequently, it was assumed that 2-propoxide surface species are generated and dehydrated at strong acid sites to propene or dehydrogenated at other active sites (medium/weak acid or strong base). Zhang and He reported a catalytic combustion mechanism of formaldehyde over TiO<sub>2</sub> catalysts with added noble metals, such as Pt, Rh, Pd, and Au [32].

In the catalytic combustion mechanism of acetaldehyde [33], the reactants acetaldehyde and oxygen molecules are adsorbed to the double active site of the catalyst to form acetic acid (AA). The formed AA migrates to the catalyst support surface with bridged oxygen and Ti<sup>4+</sup> ions, serving as Lewis acid or base active sites. The AA ions and protons generated by the dissociation of AA are strongly adsorbed onto the active sites. Finally, AA was converted to CO<sub>2</sub> and H<sub>2</sub>O by catalytic oxidation on Au/TiO<sub>2</sub>.

Yue et al. reported the reaction mechanisms for catalytic MEK combustion on Pd (-Ce)/ZSM-5 [34]. It was reported that by-products produced in the oxidation reaction were increased by the introduction of CeO<sub>2</sub>. In addition, researchers have reported that catalysts containing Ce accelerate the dehydration of the intermediate species to produce acetaldehyde and numerous secondary products.

Jiang et al. investigated the combustion of MEK on Pt/K-Al-SiO<sub>2</sub>. MEK is adsorbed over the Brønsted acid sites of Pt/K-Al-SiO<sub>2</sub> before oxidation because of the interaction with the Pt species. Subsequently, it was transformed to 2,3-butandiol and diacetyl through the intermediate products, 2-butanol and acetoin, respectively. Acetaldehyde was formed from 2,3-butandiol, and acetaldehyde and AA were formed from diacetyl conversion.

Acetaldehyde and AA undergo complete oxidation to CO<sub>2</sub> and H<sub>2</sub>O via formaldehyde and formic acid, respectively, at the Brønsted acid sites of the catalyst [35].

### 2.2.3. Other Hydrocarbons (Containing Nitrogen and Chlorine)

A study on the oxidation mechanism of hydrocarbons, including nitrogen, reported the acrylonitrile oxidation pathway using an Ag-based catalyst. Nanba et al. [36] suggested that the oxidation of acrylonitrile proceeded on Ag<sub>2</sub>O and then intermediate ammonia and acrylic acid were converted into N<sub>2</sub>, CO, and CO<sub>2</sub> on Ag metal sites. In the case of Ag/ZrO<sub>2</sub> and Ag/MgO, the catalytic oxidation of acrylonitrile over large-sized metallic Ag particles directly produced large amounts of nitrogen oxide (NO<sub>x</sub>, N<sub>2</sub>O). Meanwhile, acrylonitrile was oxidized to form nitrogen-containing products and various hydrocarbons on the active Ag phase of the Ag-ZSM-5 catalyst.

In the case of chlorine-containing hydrocarbons (trichloroethylene and chlorobenzene), Aranzabal et al. [37] evaluated the characteristics of TCE oxidation reaction over Pd/Al<sub>2</sub>O<sub>3</sub>. It was suggested that gaseous oxygen molecules are chemisorbed on the active site, and according to the E-R model, TCE can react directly with the adsorbed oxygen to form carbon oxides (CO<sub>2</sub> and CO). The catalytic oxidation of TCE has been reported to be associated with the dissociation of the C-Cl chemical bond between the catalyst and halogen. Subsequently, noble-metal-chloride species are produced on Al<sub>2</sub>O<sub>3</sub> and AlCl<sub>3</sub>. Noble-metal-chloride species are directly decomposed to Cl<sub>2</sub> and further react with TCE after being transferred onto a double bond. Dai et al. [38] proposed a catalytic oxidation mechanism for chlorobenzene over a CeO-based Ru catalyst. It was reported that the C-Cl bond in chlorobenzene decomposed relatively easily compared to the Ce<sup>3+</sup>/Ce<sup>4+</sup> active site. The final reaction was proposed as a mechanism that VOC oxidizes to CO<sub>2</sub> and H<sub>2</sub>O at surface or lattice oxygen atoms. It was reported that the catalyst was quickly deactivated by blocking of the active sites, due to the adsorption of chlorine species.

## 3. Noble-Metal-Based Catalysts for VOC Oxidation

As a catalyst for VOC removal from industrial flue gas, noble-metal-based catalysts, such as Ag, Au, Pd, Pt, Rh, and Ru, which have high activity at low temperatures, are widely used. Ceramic or metallic materials are widely used as supports for noble-metal-based catalysts. These catalysts have different VOC combustion activities depending on the type of support and bonding type with the support. However, because noble metals are expensive, studies are actively being conducted to improve the economic feasibility, stability, and selectivity of noble-metal-based catalysts by improving the catalyst dispersion, particle size, specific surface area, and structure of the active material. Furthermore, a catalyst with both high performance and economic feasibility has been developed by mixing non-noble metal catalysts possessing relatively low activity with noble metal catalysts [39].

### 3.1. Ag-Based Catalysts

VOC combustion generally occurs in the temperature range of 250–350 °C. However, it has been reported that Ag-based catalysts are less active in the oxidation of BTEX compounds in this temperature range, compared to other noble metal or transition metal catalysts. Baek et al. analyzed the characteristics of Ag catalysts during VOC combustion using Ag/HY-zeolite catalysts. As the Ag molecular content increased, the number of Ag nanoparticles increased, resulting in an increase in the catalytic activity [40].

Although the optimal content of Ag molecules reported by researchers varied significantly, it has been reported that, when Ag content is increased, the number of active sites is limited owing to the increase in the catalyst crystal size and, consequently, the decrease in specific surface area and void fraction [41].

However, according to Zhou et al., when Ag content was low, the VOC removal efficiency of the catalyst was reduced owing to the decreased content of the active phase [42]. Moreover, the Cu-Mn-Ag catalyst was impregnated onto a cordite monolith support, and the combustion efficiency of toluene was evaluated. Consequently, the catalyst activity

was the highest at 21.2 wt% Ag content, and at a relatively higher Ag content, the catalyst activity decreased because the active phase accumulated on the surface of the support.

Generally, oxygen vacancies are widely known to promote catalytic activity for VOC combustion [43–45]. Ma et al. demonstrated that the binding of Ag species was related to the benzene combustion reaction. The binding of Ag species over  $\text{CeO}_2\text{-Co}_3\text{O}_4$  induces electron transfer at the surface of the metal oxide, thus creating more active sites ( $\text{Co}^{3+}$ ) and oxygen defect sites ( $\text{Ce}^{3+}$ ) (Figure 2). This promotes the adsorption of benzene molecules on the surface of the metal oxide catalyst and the reactivity of benzene combustion at low temperatures [45].

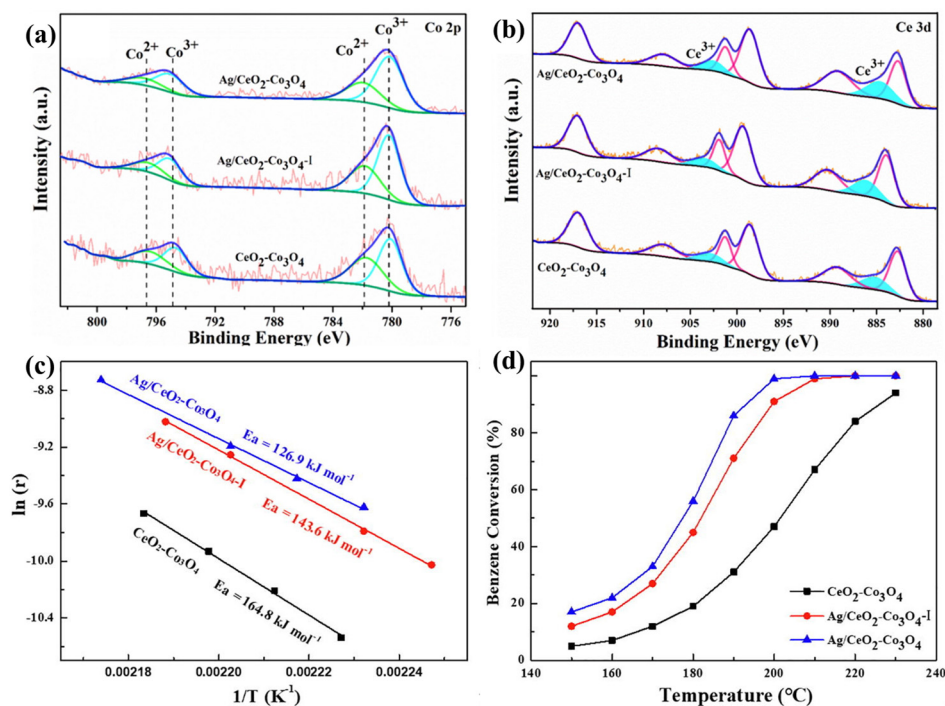


**Figure 2.** Benzene oxidation characteristics of Ag-based catalysts: XPS profiles of (a)  $\text{Co}^{2+}/\text{Co}^{3+}$  and (b)  $\text{Ce}^{3+}$ . (c) Arrhenius plot of prepared site, and (d) conversion of benzene. Reprinted with permission from ref. [45]. Copyright 2021 Elsevier.

### 3.2. Au-Based Catalysts

Gold-based catalysts are known to exhibit high oxidation activity, as reported by many previous studies [46–50]. For BTEX combustion, Au-based catalysts can react at temperatures higher than 190–400 °C, compared to Pd/Pt-based catalysts. Further, Au-based catalysts have the characteristic that they are less prone to deactivation caused by carbon coke formation inside the catalyst pores. Although Au-based catalysts have low economic efficiency compared to combustion efficiency due to the low oxygen changing rate, many studies are ongoing to address this problem by developing transition metal complexes to overcome thermal stabilities and enhance catalyst activities [51].

In particular, for Au-based catalysts in VOC combustion, the preparation method is crucial because it is highly dependent on the size of the particles and the type of support [52–55]. The mechanism of the catalytic reaction of VOC oxidation may vary depending on the type of support material used. The oxidation of VOCs is affected by the size, distribution, shape, and oxidation state of Au particles, which are the metal active sites. Many reports emphasize the role of supports and describe various supports, such as metals [23,56], aluminum [24,47,57,58], titanium [59,60], and silica [61], in Au-based catalysts. These studies optimized the shapes, sizes, contents, etc. of the Au catalyst, influencing the activity of the material in VOC oxidation, and described the correlation

between catalyst and support in heterogeneous catalysts [54,62]. Table 2 lists the VOC oxidation characteristics of the Au catalysts according to the type of support material used.

**Table 2.** Support types used with the Au active site for VOC oxidation.

Au Content (wt%)	Support	VOCs	Concentration (ppm)	T <sub>50</sub> (°C)	Ref.
1	CuO	Toluene	226	264	
1	Fe <sub>2</sub> O <sub>3</sub>	Toluene	226	307	[23]
1	Y <sub>2</sub> O <sub>3</sub>	Toluene	226	367	
1.91	Al <sub>2</sub> O <sub>3</sub>	Benzene	250	188	
2.5	CeO <sub>2</sub> /Al <sub>2</sub> O <sub>3</sub>	Benzene	250	321	[47]
7.63	3DOM LaCoO <sub>3</sub>	Toluene	1000	345	[49]
3	CeTi	Toluene	1000	130	[50]
3.2	Fe <sub>2</sub> O <sub>3</sub>	Toluene	7000	265	[46]
5.0	CeO <sub>2</sub>	Toluene	7000	370	[48]

Although some researchers have reported that the oxidation state of Au as a metal active site has an important effect on the activity of the VOC oxidation reaction, it was reported that the oxidation state is influenced by the particle size, shape, distribution, etc. of Au. Thus, research on increasing particle dispersion is in progress. Au-based catalysts are produced by various methods, such as precipitation and coprecipitation, to increase the dispersion of Au particles. It was reported that the deposition–precipitation method can produce particles in the range of 4 to 8 nm [24,63,64].

According to Carabineiro et al., metals in Au-based catalysts play a role in improving the support reducibility and catalytic reactivity. Catalyst activity is enhanced by an increase in the oxygen exchange between the lattice and the support surface. The Au/Y<sub>2</sub>O<sub>3</sub> catalyst with the Au<sup>3+</sup> oxidation state showed low catalytic activity. In contrast, for Au-based Fe<sub>2</sub>O<sub>3</sub>, NiO, and CuO catalysts, the toluene combustion activity increased with Au in the oxidation state of Au<sup>+</sup> and Au<sup>0</sup> [23].

Li et al. studied the reaction characteristics of toluene oxidation using a LaCoO<sub>3</sub> supported on a crystallized three-dimensionally ordered microporous material (3DOM). The Au-based 3DOM LaCoO<sub>3</sub> catalyst, compared to the bulk LaCoO<sub>3</sub> catalyst, possessed several characteristics, such as uniform pore size, surface thickness, and high Au dispersion [49]. In addition, it has been reported that the presence of oxygen species on the support surface promotes oxygen formation, which is advantageous for VOC oxidation.

### 3.3. Pd-Based Catalysts

Pd-based catalysts are used in a slightly higher temperature range of 200–300 °C compared to Pt-based catalysts for the VOC combustion reaction. The active phase of the Pd catalyst was Pd<sup>0</sup>, and the oxidation state of Pd affected the catalyst activity. Therefore, it has been reported that VOC combustion activity is highly dependent on the Pd content in the catalyst [65,66]. Although the chemical state of the Pd species is an important factor influencing the catalytic activity, there is controversy about this effect, as shown in Table 3.

According to Dégé et al., it was confirmed that the VOC oxidation activity was greatly affected by the Pd content and that the surface area, particle size, particle dispersion, and support also affect the activity of the catalyst [66]. Moreover, the results indicated that the coke content generated at low temperatures differed depending on the acidity of the zeolite (that is, the change in the Si/Al ratio) used as the support. For the oxidation of o-xylene (C<sub>8</sub>H<sub>10</sub>), the higher the acidity of the zeolite, the higher the rate of coke formation. Furthermore, it was confirmed that an increase in Pd content also plays a role in suppressing coke formation at the same temperature. During toluene combustion, it was determined that the stability of the Pd-based catalyst was higher than that of the Pt-based catalyst (the activated carbon fiber support was impregnated with 3.86 wt% Pt or Pd), which is advantageous for the combustion of cyclic organic compounds [67]. Bi et al. reported that a

Pd-U-H catalyst formed nanoparticles and increased the surface Pd<sup>0</sup> and lattice oxygen content. As a result of this effect, the combustion ratio of toluene was maintained at a high level in the 6-cycle reaction experiment [68].

Gil et al. examined the oxidation state of Pd according to the type of support (CeO<sub>2</sub>, TiO<sub>2</sub>, and Al<sub>2</sub>O<sub>3</sub>) through XPS analysis and evaluated the conversion rate of propene. Pd/Al<sub>2</sub>O<sub>3</sub> and Pd/TiO<sub>2</sub> have a Pd<sup>2+</sup> phase, similar to bulk PdO, whereas Pd/CeO<sub>2</sub> has a Pd<sup>4+</sup> phase. These characteristics explain the poor catalytic activity of Pd/CeO<sub>2</sub> for propene combustion because the Pd<sup>4+</sup> species form strong bonds with the support [69].

Weng et al. proposed that metallic Pd exhibited higher oxidation activity using the Pd/MgO-Al<sub>2</sub>O<sub>3</sub> catalyst system. The oxidation state of the Pd-based catalyst was characterized by XPS analysis of fresh, hydrotreated, and spent catalysts after toluene reaction. After hydrogen treatment, the Pd<sup>2+</sup> state of the catalyst increased, indicating the formation of a Pd<sup>2+</sup>/Pd<sup>0</sup> pair that aids in the toluene oxygen activity [70].

Meanwhile, a portion of the metallic Pd is oxidized to Pd<sup>2+</sup> states, and the reaction proceeds in the form of reduction aided by hydrocarbons. For Pd<sup>0</sup>, Pd<sup>2+</sup>, or mixed Pd<sup>2+</sup>/Pd<sup>0</sup> states, Pd<sup>0</sup> helps to improve the reaction rate by providing more adsorbable active sites for VOCs, and Pd<sup>2+</sup> plays a role in VOC combustion [71,72].

**Table 3.** Catalytic oxidation of VOCs over Pd catalysts with different Pd states.

Pd State	Catalyst	Used VOCs	Ref.
Pd <sup>0</sup>	Pd/CeO <sub>2</sub>	Propene	[69]
	Pd/Al <sub>2</sub> O <sub>3</sub>	Propene	
	Pd/MgO-Al <sub>2</sub> O <sub>3</sub>	Toluene	[70]
	Pd/Co <sub>3</sub> AlO	Toluene	[73]
	Pd-CoAlO-Al	Toluene	[74]
Pd <sup>0</sup> , Pd <sup>2+</sup>	Pd/HFAU(17)	o-xylene	[66]
	Pd/Ti-SBA-15	Benzene	[71]
	Pd/ZSM-5/MCM-48	Benzene	[72]
	Pd-U-EG	Toluene	[68]
	0.5%Pd/SiO <sub>2</sub>	Toluene	[75]
Pd <sup>0</sup> , Pd <sup>4+</sup>	Pd/CeO <sub>2</sub>	Propene	[69]

As the surface area and structure of the catalyst affect the activity, several researchers have investigated the oxidation states of the catalyst with relation to the support. When activated carbon is used as a support, its physical and chemical properties affect the metal deposition, dispersion, and gas adsorption efficiency [76].

Table 4 summarizes the activities of Pd-based catalysts based on different types of supports. According to Giraudon et al., the combustion performance of Pd/TiX showed superior chlorobenzene (C<sub>6</sub>H<sub>5</sub>Cl) conversion compared to Pd/ZrX. This is because the reducibility of TiO<sub>2</sub> was improved from Ti<sup>4+</sup> to Ti<sup>3+</sup> [77]. Pérez-Cadenas et al. reported that the VOC combustion reactivity of a Pd-based catalyst is affected by the surface area of mesopores, since the activity of the mesoporous supports was higher than that of the microporous and monolithic supports [78]. Mesoporous Pd/Co<sub>3</sub>O<sub>4</sub> (3D) catalysts have relatively higher activity for o-xylene oxidation than the bulk counterpart Pd/Co<sub>3</sub>O<sub>4</sub>. This improvement might be due to the increased surface exposure of PdO on the mesoporous Co<sub>3</sub>O<sub>4</sub> support [79].

Nanoparticle catalysts have different physical and chemical properties compared to single metal catalysts; thus, there is a synergistic effect in the VOC combustion properties of Pd-based catalysts [80]. Generally, alloy catalysts show a more flexible surface structure than single metal catalysts and induce affinity between the catalyst surface and the adsorbate, which contributes to high activity [81].

Comparing the reaction mechanism of Pd-Ce/Al<sub>2</sub>O<sub>3</sub> with that of Pd/Al<sub>2</sub>O<sub>3</sub>, the presence of Ce increased the active oxygen species and oxygen vacancy content on the catalyst surface. During the conversion of Ce<sup>3+</sup> to Ce<sup>4+</sup>, electrons are donated to PdO to

promote PdO to Pd, thereby generating lattice oxygens and promoting the reaction with adsorbed toluene. In addition, Ce can improve the catalyst activity by reducing the noble metal content in the catalyst [14].

Wu et al. evaluated the toluene combustion characteristics of the Au-Pd/meso-Cr<sub>2</sub>O<sub>3</sub> catalyst and reported that Au-Pd nanoparticles showed excellent toluene combustion activity, compared to single metal catalysts, owing to their strong interaction with Cr<sub>2</sub>O<sub>3</sub> [82]. Similarly, Chen et al. reported that, when a Pd-Pt-based nanoparticle catalyst was used for the benzene (C<sub>6</sub>H<sub>6</sub>) combustion reaction, it showed excellent conversion, which was due to the nano effect of the catalyst and the interaction between the active materials (Pd-Pt) [83].

**Table 4.** Comparison of Pd-based catalysts on various supports for VOC oxidation.

Active Metal	Support Material	VOCs	Temperature (°C)	Conversion (%)	Ref.
Pd	UiO-66	Toluene	200	100	[68]
	Al <sub>2</sub> O <sub>3</sub>	Toluene	252	90	[70]
	MgO-Al <sub>2</sub> O <sub>3</sub>	Toluene	209	90	[78]
	Carbon	m-Xylene	170	100	[78]
	Co <sub>3</sub> O <sub>4</sub> (3D)	o-Xylene	249	90	[79]
Pd-Ce	γ-Al <sub>2</sub> O <sub>3</sub>	Toluene	200	90	[14]
Au-Pd	Cr <sub>2</sub> O <sub>3</sub>	Toluene	165	90	[82]
Pd-Pt	Ce/γ-Al <sub>2</sub> O <sub>3</sub>	Benzene	190	95	[83]
Pd-W	TiO <sub>2</sub>	Propane	375	100	[84]

### 3.4. Pt-Based Catalysts

Pt-based catalysts are known to be the most efficient element for the combustion of cyclic hydrocarbon compounds and exhibit activity for the combustion of BTEX compounds in the temperature range of 150–350 °C [85,86]. Because the Pt-based catalyst does not interact with the support, the physical/chemical properties are maintained after impregnation. The characteristics of the support affect the deposition and dispersion of the active element, which ultimately influences the durability and poisoning resistance of the catalyst [87].

The dispersion degree of the Pt-based catalyst depends on the support, so it is important to improve this parameter to obtain high activity. Since the metal catalyst easily combines with the oxidized site of the support, the dispersibility of Pt can be improved by oxidizing the activated carbon support by acid treatment or air oxidation [88]. To improve the deposition rate of the metal catalyst onto the support, a Pt catalyst was deposited on a porous support by dry impregnation rather than wet impregnation. In addition, the ion-exchange method was used to deposit metal catalysts onto the zeolite surface [86].

Table 5 summarizes the oxidation characteristics of Pt-based catalysts using cerium oxide as a support (Pt/CeO<sub>2</sub>). It has been reported that the Pt/CeO<sub>2</sub> catalyst has superior oxygen storage capacity, reducibility, and VOC combustion performance compared to the CeO<sub>2</sub> catalyst [89]. In particular, when CeO<sub>2</sub>-Al<sub>2</sub>O<sub>3</sub> was used as a support, the Pt catalyst formed nanoparticles and exhibited high reducibility and activity in xylene and toluene oxidation. In addition, owing to the improvement in the dispersion degree of Pt particles, the high temperature (>300 °C) oxidation activity might be increased [90]. The catalyst using Al<sub>2</sub>O<sub>3</sub>-CeO<sub>2</sub> as a support exhibited improved oxidation of dichloromethane (DCM, CH<sub>2</sub>Cl<sub>2</sub>) [91]. The addition of Ce and Pt catalysts enhanced the selectivity of CO<sub>2</sub> and inhibits catalyst deactivation by reducing the formation of CH<sub>3</sub>Cl, CH<sub>2</sub>O, CO, etc.

The activity of the catalyst for VOC oxidation was greatly affected by the type and shape of the catalyst support. The surface oxygen vacancies, which play an important role in adsorbing gaseous oxygen and promoting combustion activity, depend on shape of catalyst. Peng et al. [92] prepared catalysts by adding Pt catalysts to CeO<sub>2</sub> supports with various crystal sizes. A high-efficiency Pt/CeO<sub>2</sub> catalyst was optimized for toluene combustion by controlling the degree of exposure of the support surface and the role of CeO<sub>2</sub> was reported.

**Table 5.** Comparison of Pt-based catalysts on various supports for VOC oxidation.

Pt Content (wt%)	Support	VOCs	Concentration (ppm)	Temperature (°C)	T <sub>90</sub> (°C)	Ref.
1	CeO <sub>2</sub>	Benzene	2.0 g/m <sup>3</sup>	125/150	153	[89]
1	Al <sub>2</sub> O <sub>3</sub> -CeO <sub>2</sub> (30%)	Toluene	2500	160/220	<250	[90]
1.3	Al <sub>2</sub> O <sub>3</sub> -CeO <sub>2</sub> (23%)	DCM	500	320/375	375	[91]
0.2	CeO <sub>2</sub> -r	Toluene	1000	138/150	150	
0.2	CeO <sub>2</sub> -p	Toluene	1000	168/190	175	[92]
0.2	CeO <sub>2</sub> -c	Toluene	1000	153/175	190	

Recently, many studies have been reported on the combustion of chlorinated volatile organic compounds (CVOCs). As a result of evaluating the support of the Pt-based catalysts used for DOM combustion, the activity of Pt/Al<sub>2</sub>O<sub>3</sub> was superior compared to that of Pt/TiO<sub>2</sub>, Pt/CeO<sub>2</sub>, and Pt/MgO. This is because when Al<sub>2</sub>O<sub>3</sub> is used as a support, the particle size of Pt is reduced to less than 1.2 nm [93].

Pt molecules serve to increase the number of weak acid sites and reduce the number of strong acid sites on the catalyst surface. This phenomenon strengthens the adsorption strength between the VOCs and the catalyst surface. Yang et al. confirmed that an insufficient active oxygen supply was improved by adding Pt to the Pd/CeO<sub>2</sub>/γ-Al<sub>2</sub>O<sub>3</sub> catalyst in the oxidation of various VOCs [94].

### 3.5. Rh-Based Catalysts

It is known that Rh-based VOC combustion catalysts are far less explored than other novel metal-based catalysts. Recently, they have attracted attention because of their improved effects on the catalytic oxidation of CVOCs, aromatics, and alkanes.

Rh-based catalysts have high stability with the support material compared to other noble metal catalysts (Ru, Rh, Pd, and Pt) [91,95]. Noble metals have high thermal stability while forming an M–O–Ce bond with a CeO<sub>2</sub> support. Saburo et al. reported that the M–O–Ce bond was maintained above 800 °C for Ru- and Pd-based catalysts, while the M–O–Ce bond endured below 500 °C, and Ru was present as bulk RuO<sub>2</sub> below 500 °C. Therefore, it was concluded that the stability between noble metals and the CeO<sub>2</sub> support was high and followed the order of Rh > Pd > Pt > Ru [96].

According to Pitkäaho et al. in Table 6, the Rh-based catalytic activity sequence with different supports was Al<sub>2</sub>O<sub>3</sub> > Al<sub>2</sub>O<sub>3</sub>-CeO<sub>2</sub> > Al<sub>2</sub>O<sub>3</sub>-TiO<sub>2</sub>. When the same support was used, the Rh-based catalyst exhibited higher activity than other metal-based catalysts (Pd, V<sub>2</sub>O<sub>5</sub>, and Pt). For the combustion of CVOCs, selectivity to CO, CO<sub>2</sub>, HCl, and high activity are required. The addition of Rh improved the HCl yield of the Al<sub>2</sub>O<sub>3</sub> supported catalyst and had a HCl selectivity of 93%. For the Rh catalyst, the amount of CO formed differed depending on the support. It showed a high CO yield of 46% over the Al<sub>2</sub>O<sub>3</sub> supported catalysts, 14% over Rh/Al<sub>2</sub>O<sub>3</sub>-TiO<sub>2</sub>, and 1% over Rh/Al<sub>2</sub>O<sub>3</sub>-CeO<sub>2</sub> [91].

**Table 6.** Comparison of Rh-based catalysts on various supports for VOC oxidation.

Rh Content (wt%)	Support	VOCs	Concentration (ppm)	T <sub>90</sub> (°C)	CO <sub>2</sub> Yield (%)	Ref.
0.5	Al <sub>2</sub> O <sub>3</sub> -TiO <sub>2</sub>	DCM	500	360	85 (at 660 °C)	
0.5	Al <sub>2</sub> O <sub>3</sub> -CeO <sub>2</sub>	DCM	500	380	40 (at 600 °C)	[91]
1	CeO <sub>2</sub>	Toluene	7000	375	100 (at 590 °C)	
1	TiO <sub>2</sub>	Chlorobenzene	500	339	95 (at 400 °C)	[97]

In the reports on Rh-based catalysts, Rh/TiO<sub>2</sub> yielded the lowest Cl content of 0.61% after CVOc oxidation, which was consistent with the amount of polychlorinated by-products (dichlorobenzene, trichlorobenzene, tetra-chlorobenzene, pent-chlorobenzene, etc.) detected by XPS analyses. The maximum concentration of chlorobenzene combustion by-products, 1,3-dichlorobenzene and 1,4-dichlorobenzene, reached 23 ppm at 310 °C [97].

We can now summarize the contents of verse 3, although the combustion characteristics of VOCs depend on the support; the characteristics of Pd, Pt, and Rh catalysts supported on TiO<sub>2</sub> were examined in the oxidation of chlorobenzene, as shown in Figure 3 [97]. For all three catalysts, the oxidation of chlorobenzene is initiated at 250 °C, and all of them exhibit a conversion rate of more than 95% at temperatures above 350 °C.: (1) T<sub>90</sub> (Pd/TiO<sub>2</sub>) = 340 °C, (2) T<sub>90</sub> (Pt/TiO<sub>2</sub>) = 337 °C, and (3) T<sub>90</sub> (Rh/TiO<sub>2</sub>) = 339 °C. In particular, Pt/TiO<sub>2</sub> exhibited higher low-temperature catalytic activity than those of Pd/TiO<sub>2</sub> and Rh/TiO<sub>2</sub>. According to the evaluation of the CO<sub>x</sub> concentration, the CO yield was lower than 1%, which indicated that CO<sub>2</sub> selectivity was high. The generated trend for the by-products (PhCl<sub>2</sub>, PhCl<sub>3</sub>, PhCl<sub>4</sub>, etc.) is shown in Figure 3b. The maximum amounts of by-products are 65 ppm, 88 ppm, and 100 ppm at 360 °C, 340 °C, and 340 °C for Pt/TiO<sub>2</sub>, Pd/TiO<sub>2</sub> and Rh/TiO<sub>2</sub>, respectively. The Pt-based catalyst exhibited high VOC oxidation activity at temperatures ≤ 300 °C, and the use of the Rh-based catalyst was advantageous at temperatures ≥ 370 °C.

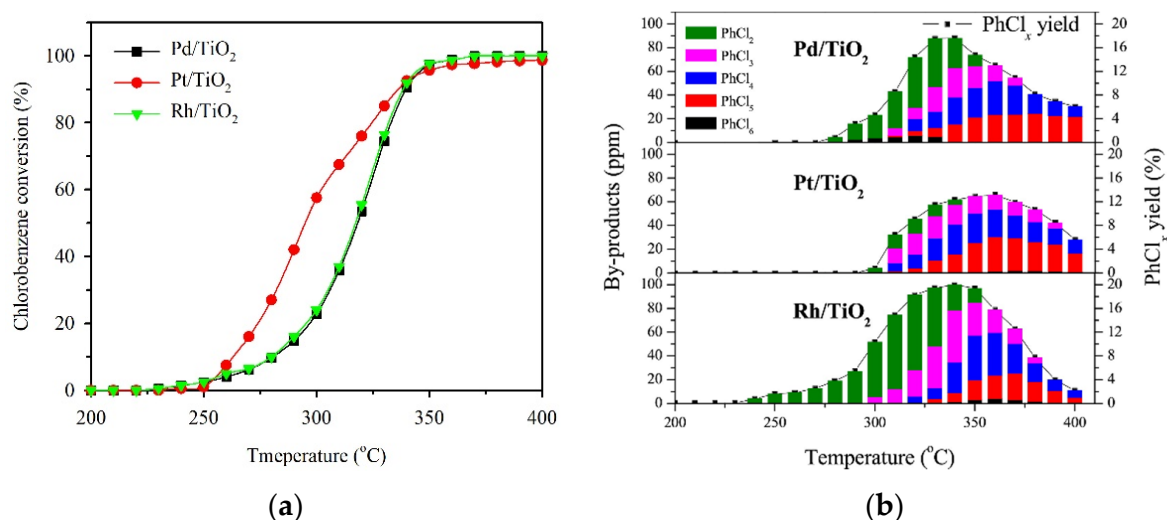


**Figure 3.** Conversion over Pd/TiO<sub>2</sub>, Pt/TiO<sub>2</sub>, Rh/TiO<sub>2</sub>: (a) chlorobenzene conversion and (b) by-product yields. Reprinted with permission from ref. [97]. Copyright 2019 Elsevier.

As mentioned above, most research on VOC oxidation over noble metals used Pt or Pd, which were manufactured using supports, such as TiO<sub>2</sub>, CeO<sub>2</sub>, Al<sub>2</sub>O<sub>3</sub>, and ZrO<sub>2</sub>. It has been reported that the acid–base properties of the support typically play an important role in catalyst performance. In particular, the Pd-based catalyst has been reported to have excellent durability in the catalytic oxidation of chlorinated VOCs. Meanwhile, some researchers have reported that a combination of Pt and Pd achieved higher VOC oxidation efficiency compared to that of single metal catalysts. In the oxidation reaction over noble metal catalysts, catalytic performance varies depending on the components of VOCs and supports. Therefore the main catalyst should be selected according to their application, such as the operation temperature, VOCs concentration, and components.

## 4. Deactivation and Regeneration

### 4.1. Catalyst Poisoning and Deactivation

For industrial applications, VOC catalysts should exhibit high catalytic activity and stability. Noble metal VOC catalysts have high combustion activities, but catalysts may suffer from deactivation (via coking, poisoning, thermal sintering, etc.) of the catalysts. Nitride, chloride, and water vapor cause poisoning of the catalysts, by disabling the active sites in the catalytic combustion of VOCs.

In general, water vapor is present in most flue gases and are produced by VOC combustion reactions. Water vapor has two competing effects, either promoting VOC

combustion or poisoning the catalyst [98,99]. When water molecules are adsorbed on the catalyst surface, they may induce the generation of -OH components over the catalyst by dissociation of H<sub>2</sub>O, and additional water molecules are adsorbed through hydrogen bonding to form multi-layered water molecules. This phenomenon has two competing effects on VOC combustion. The positive effect is that the water molecules serve as a precursor of -OH to promote combustion, whereas the negative effect is that the adsorbate (water molecules) competes with VOC molecules for the active surface sites. Therefore, it is possible to optimize the water vapor effect by compromising the above competitive effects [100].

He et al. examined the effect of water vapor on the mineralization and deactivation of a VOC oxidation catalyst. The oxidation activity of VOCs is highly dependent on their hydrophobic and hydrophilic properties because they must pass through the multilayer of adsorbed water to approach the catalyst active sites.

For example, hydrophilic VOCs, such as n-propionaldehyde, n-propanol, and n-propylamine, can easily pass through the water layers to approach the catalyst surface. Meanwhile, hydrophobic VOCs, such as n-propanethiol and n-chloropropane, experience an inhibitory effect attributed to the hydrous multilayer of adsorbed water molecules [101].

CVOCs can poison catalysts by oxidizing to form chlorine, chlorides, and HCl. Chlorine partially blocks the active sites of the catalyst and the formation of active oxychlorinated species. In addition, Cl can inhibit catalyst activity by strong adsorption [102]. The chlorine produced by CVOC combustion can be converted to HCl through the Deacon reaction, which is the combustion reaction of chlorinated volatile organic compounds [103].

Cen et al. investigated the Cl species deactivation effect on CeO<sub>2</sub> (1 1 1) catalyst surfaces and identified their selectivity to HCl and Cl<sub>2</sub>. In the combustion process of CVOCs, the higher the O<sub>2</sub>/Cl ratio in the feed gas, the more inhibited the deactivation of the catalysts. Therefore, the introduction of the H-containing component helps to convert Cl species to HCl rather than Cl<sub>2</sub>. In this regard, water can improve the selectivity of HCl/Cl<sub>2</sub> produced by the Deacon reaction. It should be noted that competitive adsorption between water vapor and oxygen may lead to the loss of catalyst activity at low temperatures [104]. Zhao et al. studied the influence of water on 1,2-dichlorobenzene combustion and analyzed the catalyst deactivation mechanism caused by water vapor [105]. Qiguang et al. reported that, in the combustion of DCM over P/CeO<sub>2</sub> and Ru/CeO<sub>2</sub> catalysts (as shown in Figure 4), the presence of water inhibits the formation of intermediates, which results in an inhibitory effect of DCM oxidation. It was confirmed that hydrogenation and dichlorination occurred when a P/CeO<sub>2</sub> catalyst was used in flue gas after the reaction, and chlorination and dehydrogenation occurred when a Ru/CeO<sub>2</sub> catalyst was used. It was reported less that catalyst deactivation occurred when Ru was present in the catalyst [106].

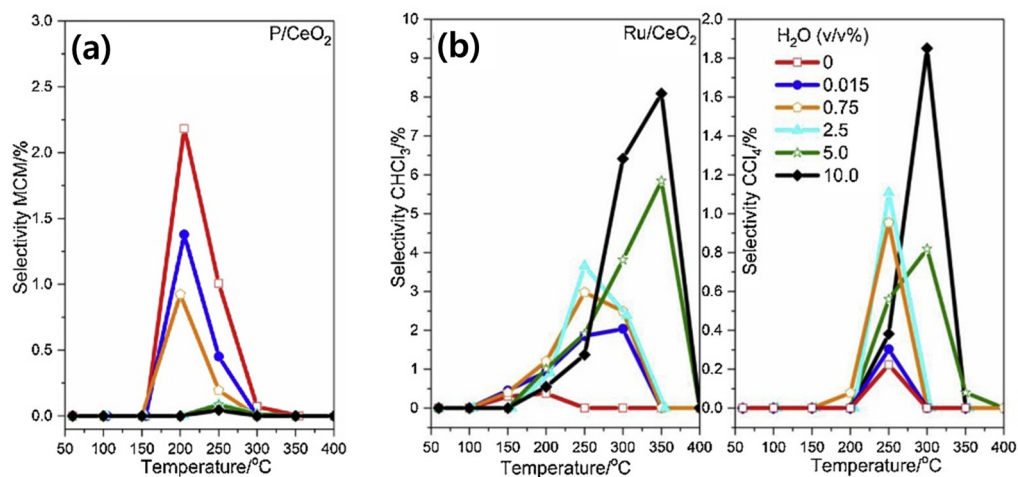


**Figure 4.** (a,b) Deactivation effect of catalysts by H<sub>2</sub>O in CVOC oxidation by analyzing by-products using P/CeO<sub>2</sub> and Ru/CeO<sub>2</sub>. Reprinted with permission from ref. [106]. Copyright 2019 Elsevier.

Nitrogen-containing VOCs (NVOCs) form intermediates, such as NO, N<sub>2</sub>O, NH<sub>3</sub>, and HCN, which easily cause catalyst deactivation. Pd catalysts have been reported to be unsuitable for use in the nitrile oxidation of VOCs because they produce undesirable NO<sub>x</sub> gases [107].

#### 4.2. Catalyst Regeneration

An ideal VOC combustion catalyst is expected to have high combustion efficiency, easy regeneration, fast combustion rate, and high thermal and hydrothermal stability [22]. Although noble metal catalysts have high catalytic activity, they may suffer from deactivation (coking, poisoning, thermal sintering, and catalyst volatilization). These factors cause a decrease in the number of active sites, surface area, and plug pores, leading to deactivation of the catalyst [108].

The ability of catalyst regeneration depends on the reversibility of the deactivation process. Deactivated catalysts can be regenerated by several methods, such as heat treatment, chemical regeneration, ozone oxidation, plasma treatment, stripping, or supplying air [109–111]. When deactivated by carbon deposition or coking, it can be regenerated relatively easily by gasification with hydrogen, oxygen, water, or air at the required temperature [112–114]. Catalyst sintering is generally irreversible. However, some noble metal catalysts can be expected to recover VOC combustion efficiency by metal redispersion.

However, for the elimination of CVOCs, it is difficult to find an effective regeneration and reuse method for deactivated catalysts. The formation of volatile metal oxyhydrochloride may lead to irreversible deactivation of the catalyst, in which the active phase is volatilized. Zhang et al. investigated the correlation between catalyst deactivation and physicochemical properties through experiments of the reaction–regeneration cycle using a LaMnO<sub>3</sub> perovskite catalyst [110]. With regeneration, the specific surface area and adsorbed oxygen concentration decreased, which was proposed to be due to the effect of the decrease in Mn<sup>4+</sup> content on the surface of the catalyst. Therefore, the mobility of surface oxygen and the activation of gaseous oxygen was reduced; thus, the catalyst activity is lowered even after regeneration [115].

Oliveira et al. confirmed that, in the combustion of chlorobenzene and xylene using a catalyst prepared by impregnating Cr in bentonite, Cr reacted with HCl, Cl<sub>2</sub>, etc. to generate volatile compounds of CrO<sub>2</sub>Cl<sub>2</sub> and the active species were lost [116]. When catalysts, such as Pt/TiO<sub>2</sub>, Pd/TiO<sub>2</sub>, and Ru/TiO<sub>2</sub>, were used for the combustion of DCM, -Cl species were adsorbed on the catalyst surface. The adsorbate altered the chemical structure and composition at the active site to generate inactive chlorine compounds, such as PdCl<sub>2</sub>, PdCl<sub>4</sub>, and PtCl<sub>4</sub> [108].

The reproducibility of these catalysts can be determined by several factors, such as irreversible volatilization of the active species, changes in physicochemical state, reversible chlorination, sintering, and carbon deposition. Catalysts deactivated by reversible factors can be regenerated relatively easily. In addition, the presence of water vapor during regeneration helps to remove coke and chlorine, which makes moist air more favorable for catalyst regeneration than dry air [117]. Cuicui et al. reported that the oxidation of CVOCs occurs on the catalyst and H<sub>2</sub>O removes adsorbed chlorine through the mechanism shown in Figure 5 [118].

Pengfei et al. explored the regeneration performance and mechanism of a bimetal H-zeolite catalyst (Cu-Nb/HZSM-5) for chlorobenzene combustion. Chlorobenzene combustion occurred on the Brønsted acid sites and active copper sites. Therefore, the reason for catalyst deactivation was the formation of copper chloride and surface coke, which resulted in a loss of Brønsted acid sites. Catalyst recovery was mostly possible by converting the coke to saturated hydrocarbons or CO<sub>2</sub> via isothermal regeneration in air at 400 °C. In addition, copper hydrochloride can be transformed into copper oxide by the Deacon reaction with surface lattice oxygens. In particular, by supplying water vapor, the chloride and coke adsorbed on the catalyst can be comprehensively removed by further hydrolysis [119].

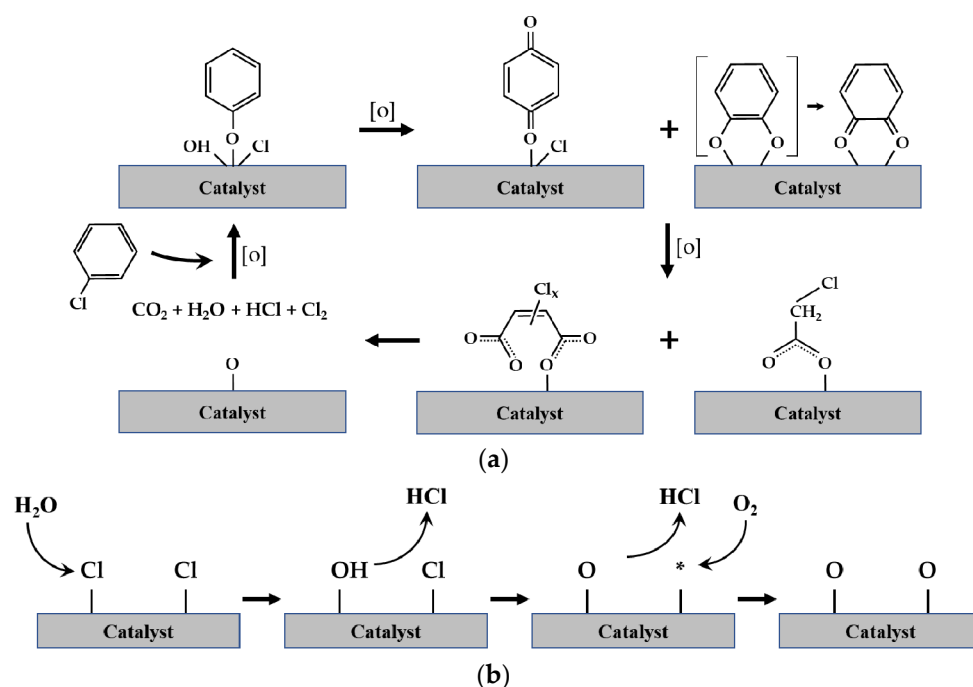


**Figure 5.** (a) Oxidation and (b) regeneration of catalysts by the H<sub>2</sub>O mechanism of CVOs.

Currently, many catalysts that can be regenerated using heat treatment and mechanical methods are being developed. However, methodological limitations arise when irreversible catalyst deactivation occurs, and studies are being conducted to overcome this material limitation through process optimization, such as the supply of moisture.

## 5. Conclusions

Catalytic oxidation is used as an effective method to treat VOCs emitted by various industrial sites. Various catalysts, such as noble metals, non-noble metals, and perovskites, have been investigated for the catalytic combustion of VOCs. Noble metal catalysts are one of the most effective materials because they can be applied to VOC combustion at lower temperatures compared to other materials. The catalyst activity depends on the type of active material and the characteristics of the support. In addition, the particle size, pore size, specific surface area, structure, strength of acid sites, etc., according to the preparation method of the catalyst, may affect VOC combustion activity. This research field continues to be active. In this review, we describe recent trends in the catalytic oxidation of VOCs using noble metal catalysts. Most of the research published to date has focused on achieving remarkable results through catalyst design for low-temperature VOC combustion. Materials based on non-noble metals, such as Ce, Cu, and Mn, which are often used as supports for noble metals, have been considerably studied due to their inherent catalytic activity. However, the addition of noble metal catalysts improves VOC combustion performance at low temperatures. Nevertheless, studies on the development of catalysts for various VOC components and overcoming deactivation due to sintering, coking, and chlorine/sulfur/water poisoning are still insufficient. Therefore, additional studies related to the development of catalysts for various VOC components and the interpretation of catalyst deactivation mechanisms are required.

**Author Contributions:** H.-S.K., H.-J.K. and J.-H.K. (Ji-Hyeon Kim) jointly collected the literature and equally contributed to this review. S.-H.K., J.-H.K. (Jin-Ho Kim), N.-K.P. and D.-S.Y. helped with data collection. J.-H.R. and J.-W.B. revised the draft and supervised the work. All authors have read and agreed to the published version of the manuscript.

**Funding:** This work was supported by the Korea Ministry of Environment as “The reduction management program of fine dust blind spot” (Project No. 202003060012). This research was supported by the Ministry of Trade, Industry & Energy (MOTIE), Korea Evaluation Institute of Industrial Technology (KEIT) (Project No. 20015460).

**Data Availability Statement:** Not applicable.

**Conflicts of Interest:** The authors declare no conflict of interest.

## References

1. US EPA. Technical Overview of Volatile Organic Compounds. Available online: <https://www.epa.gov/indoor-air-quality-iaq/technical-overview-volatile-organic-compounds> (accessed on 2 September 2021).
2. Liu, Y.; Han, F.; Liu, W.; Cui, X.; Luan, X.; Cui, Z. Process-based volatile organic compound emission inventory establishment method for the petroleum refining industry. *J. Clean. Prod.* **2020**, *263*, 121609. [CrossRef]
3. Meng, L.; Qiang, Z.; Bo, Z.; Dan, T.; Yu, L.; Fei, L.; Chaopeng, H.; Sicong, K.; Liu, Y.; Yuxuan, Z.; et al. Persistent growth of anthropogenic non-methane volatile organic compound (NMVOC) emissions in China during 1990–2017: Drivers, speciation and ozone formation potential. *Atmos. Chem. Phys.* **2019**, *19*, 8897–8913.
4. Brown, G.S.; Frankel, A.; Hafner, H.R. Source apportionment of VOCs in the Los Angeles area using positive matrix factorization. *Atmos. Environ.* **2007**, *41*, 227–237. [CrossRef]
5. National Air Emission Inventory and Research Center. Emissions by Source Category. 2018. Available online: <https://www.air.go.kr/en/jbagg/sub03-1> (accessed on 14 September 2021).
6. Park, N.K.; Kwon, B.C.; Kang, D.; Yun, D.; Ryu, J.H.; Kang, S.H. Characteristics of Catalytic Combustion with VOCs Species Emitted in Printing Process. *J. Energy Clim. Change* **2020**, *15*, 81–91.
7. Kim, H.C.; Kim, S.; Kim, B.-U.; Jin, C.-S.; Hong, S.; Park, R.; Son, S.-W.; Bae, C.; Bae, M.; Song, C.-K.; et al. Recent increase of surface particulate matter concentrations in the Seoul Metropolitan Area, Korea. *Sci. Rep.* **2017**, *7*, 1–7. [CrossRef]
8. Zhang, X.; Gao, B.; Creamer, A.E.; Cao, C.; Li, Y. Adsorption of VOCs onto engineered carbon materials: A review. *J. Hazard. Mater.* **2017**, *15*, 102–123. [CrossRef] [PubMed]
9. Guo, Y.; Wen, M.; Li, G.; An, T. Recent advances in VOC elimination by catalytic oxidation technology onto various nanoparticles catalysts: A critical review. *Appl. Catal. B* **2021**, *281*, 119447. [CrossRef]
10. Kang, S.W.; Min, B.H.; Suh, S.S. A study on cleaning Process for Benzene Recovery in Activated Carbon bed. *J. Kor. Oil Chem. Soc.* **2002**, *19*, 108–116.
11. Deng, J.; He, S.; Xie, S.; Yang, H.; Liu, Y.; Guo, G.; Dai, H. Ultralow Loading of Silver Nanoparticles on Mn<sub>2</sub>O<sub>3</sub> Nanowires Derived with Molten Salts: A High-Efficiency Catalyst for the Oxidative Removal of Toluene. *Environ. Sci. Technol.* **2015**, *49*, 11089–11095. [CrossRef] [PubMed]
12. Liu, Y.; Dai, H.; Deng, J.; Xie, S.; Yang, H.; Tan, W.; Han, W.; Jiang, Y.; Guo, G. Mesoporous Co<sub>3</sub>O<sub>4</sub>-supported gold nanocatalysts: Highly active for the oxidation of carbon monoxide, benzene, toluene, and o-xylene. *J. Catal.* **2014**, *309*, 408–418. [CrossRef]
13. Alejo, A.; Esteban, L.F.; Aline, V.; Sebastián, E.C. Identification of key reaction intermediates during toluene combustion on a Pd/CeO<sub>2</sub> catalyst using operando modulated DRIFT spectroscopy. *Catal. Today* **2021**, in press.
14. He, C.; Li, P.; Cheng, J.; Hao, Z.-P.; Xu, Z.-P. A Comprehensive Study of Deep Catalytic Oxidation of Benzene, Toluene, Ethyl Acetate, and their Mixtures over Pd/ZSM-5 Catalyst: Mutual Effects and Kinetics. *Water Air Soil Pollut.* **2009**, *209*, 365–376. [CrossRef]
15. Ren, S.; Liang, W.; Li, Q.; Zhu, Y. Effect of Pd/Ce loading on the performance of Pd-Ce/ $\gamma$ -Al<sub>2</sub>O<sub>3</sub> catalysts for toluene abatement. *Chemosphere* **2020**, *251*, 126382. [CrossRef]
16. Bedia, J.; Rosas, J.M.; Rodríguez-Mirasol, J.; Cordero, T. Pd supported on mesoporous activated carbons with high oxidation resistance as catalysts for toluene oxidation. *Appl. Catal. B Environ.* **2010**, *94*, 8–18. [CrossRef]
17. Aranzabal, A.; González-Marcos, J.A.; López-Fonseca, R.; Gutiérrez-Ortiz, M.A.; González-Velasco, J.R. Deep catalytic oxidation of chlorinated VOC mixtures from groundwater stripping emissions. *Stud. Surf. Sci. Catal.* **2000**, *130*, 1229–1234.
18. Radic, N.; Grbic, B.; Terlecki-Baricevic, A. Kinetics of deep oxidation of n-hexane and toluene over Pt/Al<sub>2</sub>O<sub>3</sub> catalysts: Platinum crystallite size effect. *Appl. Catal. B* **2004**, *50*, 153–159. [CrossRef]
19. Ordóñez, S.; Bello, L.; Sastre, H.; Rosal, R.; Díez, F.V. Kinetics of the deep oxidation of benzene, toluene, n-hexane and their binary mixtures over a platinum on  $\gamma$ -alumina catalyst. *Appl. Catal. B* **2002**, *38*, 139–149. [CrossRef]
20. Banu, I.; Manta, C.M.; Bercaru, G.; Bozga, G. Combustion kinetics of cyclooctane and its binary mixture with o-xylene over a Pt/ $\gamma$ -alumina catalyst. *Chem. Eng. Res. Des.* **2015**, *102*, 399–406. [CrossRef]
21. Chang, S.; Jia, Y.; Zeng, Y.; Qian, F.; Guo, L.; Wu, S.; Lu, J.; Han, Y. Effect of inter-action between different CeO<sub>2</sub> plane and platinum nanoparticles on catalytic activity of Pt/CeO<sub>2</sub> in toluene oxidation. *J. Rare Earths* **2021**, in press. [CrossRef]
22. Yang, C.; Miao, G.; Pi, Y.; Xia, Q.; Wu, J.; Li, Z.; Xiao, J. Abatement of various types of VOCs by adsorption/catalytic oxidation: A review. *Chem. Eng. J.* **2019**, *370*, 1128–1153. [CrossRef]
23. Carabineiro, S.; Chen, X.; Martynyuk, O.; Bogdanchikova, N.; Avalos-Borja, M.; Pestryakov, A.; Tavares, P.; Órfão, J.; Pereira, M.F.; Figueiredo, J. Gold supported on metal oxides for volatile organic compounds total oxidation. *Catal. Today* **2015**, *244*, 103–114. [CrossRef]

24. Gluhoi, A.C.; Bogdanchikova, N.; Nieuwenhuys, B.E. The effect of different types of additives on the catalytic activity of Au/Al<sub>2</sub>O<sub>3</sub> in propene total oxidation: Transition metal oxides and ceria. *J. Catal.* **2005**, *229*, 154–162. [[CrossRef](#)]
25. Arzamendi, G.; O'Shea, V.A.D.; Álvarez-Galván, M.C.; Fierro, J.L.G.; Arias, P.L.; Gandía, L.M. Kinetics and Selectivity of Methyl-Ethyl-Ketone Combustion in Air over Alumina-Supported PdOx-MnOx Catalysts. *J. Catal.* **2009**, *261*, 50–59. [[CrossRef](#)]
26. Jabłońska, M.; Król, A.; Kukulska-Zajac, E.; Tarach, K.A.; Girman, V.; Chmielarz, L.; Góra-Marek, K. Zeolites Y modified with palladium as effective catalysts for low-temperature methanol incineration. *Appl. Catal. B Environ.* **2015**, *166–167*, 353–365. [[CrossRef](#)]
27. Almukhlifi, H.A.; Burns, R.C. The Complete Oxidation of iso-Butane over CeO<sub>2</sub> and Au/CeO<sub>2</sub>, and the Composite Catalysts MOx/CeO<sub>2</sub> and Au/MOx/CeO<sub>2</sub> (Mn<sup>+</sup> = Mn, Fe, Co and Ni): The Effects of Gold Nanoparticles Obtained from n-Hexanethiolate-Stabilized Gold Nanoparticles. *J. Mol. Catal. A Chem.* **2016**, *415*, 131–143. [[CrossRef](#)]
28. Garetto, T.F.; Rincón, E.; Apesteguía, C.R. Deep oxidation of propane on Pt-supported catalysts: Drastic turnover rate enhancement using zeolite supports. *Appl. Catal. B Environ.* **2004**, *48*, 167–174. [[CrossRef](#)]
29. Yang, H.L.; Ma, C.Y.; Zhang, X.; Li, Y.; Cheng, J.; Hao, Z.P. Understanding the Active Sites of Ag/Zeolites and Deactivation Mechanism of Ethylene Catalytic Oxidation at Room Temperature. *ACS Catal.* **2018**, *8*, 1248–1258. [[CrossRef](#)]
30. Wan, J.; Ran, R.; Li, M.; Wu, X.; Weng, D. Effect of acid and base modification on the catalytic activity of Pt/Al<sub>2</sub>O<sub>3</sub> for propene oxidation. *J. Mol. Catal. A Chem.* **2014**, *383–384*, 194–202. [[CrossRef](#)]
31. Liu, S.Y.; Yang, S.M. Complete oxidation of 2-propanol over gold-based catalysts supported on metal oxides. *Appl. Catal. A Gen.* **2008**, *334*, 92–99. [[CrossRef](#)]
32. Zhang, C.; He, H. A comparative study of TiO<sub>2</sub> supported noble metal catalysts for the oxidation of formaldehyde at room temperature. *Catal. Today* **2007**, *126*, 345–350. [[CrossRef](#)]
33. Nikawa, T.; Naya, S.-I.; Kimura, T.; Tada, H. Rapid removal and subsequent low-temperature mineralization of gaseous acetaldehyde by the dual thermocatalysis of gold nanoparticle-loaded titanium(IV) oxide. *J. Catal.* **2015**, *326*, 9–14. [[CrossRef](#)]
34. Yue, L.; He, C.; Zhang, X.Y.; Li, P.; Wang, Z.; Wang, H.L.; Hao, Z.P. Catalytic Behavior and Reaction Routes of MEK Oxidation over Pd/ZSM-5 and Pd-Ce/ZSM-5 Catalysts. *J. Hazard. Mater.* **2013**, *244–245*, 613–620. [[CrossRef](#)]
35. Jiang, Z.Y.; He, C.; Dummer, N.F.; Shi, J.W.; Tian, M.J.; Ma, C.Y.; Hao, Z.P.; Taylor, S.H.; Ma, M.D.; Shen, Z.X. Insight into the Efficient Oxidation of Methyl-Ethyl-Ketone over Hierarchically Micro-Mesostructured Pt/K-(Al)SiO<sub>2</sub> Nanorod Catalysts: Structure-Activity Relationships and Mechanism. *Appl. Catal. B* **2019**, *226*, 220–233. [[CrossRef](#)]
36. Nanba, T.; Masukawa, S.; Uchisawa, J.; Obuchi, A. Effect of Support Materials on Ag Catalysts Used for Acrylonitrile Decomposition. *J. Catal.* **2008**, *259*, 250–259. [[CrossRef](#)]
37. Aranzabal, A.; Ayastuy-Arizti, J.L.; González-Marcos, J.A.; González-Velasco, J.R. The Reaction Pathway and Kinetic Mechanism of the Catalytic Oxidation of Gaseous Lean TCE on Pd/Alumina Catalysts. *J. Catal.* **2003**, *214*, 130–135. [[CrossRef](#)]
38. Dai, Q.G.; Bai, S.X.; Wang, X.Y.; Lu, G.Z. Catalytic Combustion of Chlorobenzene over Ru-Doped Ceria Catalysts: Mechanism Study. *Appl. Catal. B* **2013**, *129*, 580–588. [[CrossRef](#)]
39. Yang, Z.; Yuxi, L.; Shaohua, X.; Haibao, H.; Guangsheng, G.; Hongxing, D.; Jiguang, D. Supported ceria-modified silver catalysts with high activity and stability for toluene removal. *Environ. Int.* **2019**, *128*, 335–342.
40. Baek, S.W.; Kim, J.R.; Ihm, S.K. Design of dual functional adsorbent/catalyst system for the control of VOC's by using metal-loaded hydrophobic Y-zeolites. *Catal. Today* **2004**, *93–95*, 575–581. [[CrossRef](#)]
41. Kim, S.C.; Ryu, J.Y. Properties and performance of silver-based catalysts on the catalytic oxidation of toluene. *Environ. Tech.* **2011**, *32*, 561–568. [[CrossRef](#)]
42. Zhou, J.C.; Wu, D.F.; Jiang, W.D.; Li, Y.D. Catalytic combustion of toluene over a copper-manganese-silver mixedoxide catalyst supported on a washcoated ceramic monolith. *Chem. Eng. Technol.* **2009**, *32*, 1520–1526. [[CrossRef](#)]
43. Hou, J.; Liu, L.; Li, Y.; Mao, M.; Lv, H.; Zhao, X. Tuning the K<sup>+</sup> Concentration in the Tunnel of OMS-2 Nanorods Leads to a Significant Enhancement of the Catalytic Activity for Benzene Oxidation. *Environ. Sci. Technol.* **2013**, *47*, 13730–13736. [[CrossRef](#)]
44. Jiang, W.; Feng, Y.; Zeng, Y.; Yao, Y.; Gu, L.; Sun, H.; Ji, W.; Arandiyán, H.; Au, C.-T. Establishing high-performance Au/cobalt oxide interfaces for low-temperature benzene combustion. *J. Catal.* **2019**, *375*, 171–182. [[CrossRef](#)]
45. Ma, X.; Xiao, M.; Yang, X.; Yu, X.; Ge, M. Boosting benzene combustion by engineering oxygen vacancy-mediated Ag/CeO<sub>2</sub>-Co<sub>3</sub>O<sub>4</sub> catalyst via interfacial electron transfer. *J. Colloid Interface Sci.* **2021**, *594*, 882–890. [[CrossRef](#)] [[PubMed](#)]
46. Minicò, S.; Scirè, S.; Crisafulli, C.; Maggiore, R.; Galvagno, S. Catalytic combustion of volatile organic compounds on gold/iron oxide catalysts. *Appl. Catal. B Environ.* **2000**, *28*, 245–251. [[CrossRef](#)]
47. Centeno, M.A.; Paulis, M.; Montes, M.; Odriozola, J.A. Catalytic combustion of volatile organic compounds on Au/CeO<sub>2</sub>/Al<sub>2</sub>O<sub>3</sub> and Au/Al<sub>2</sub>O<sub>3</sub> catalysts. *Appl. Catal. A Gen.* **2002**, *234*, 65–78. [[CrossRef](#)]
48. Scirè, S.M.S.; Minicò, S.; Crisafulli, C.; Satriano, C.; Pistone, A. Catalytic combustion of volatile organic compounds on gold/cerium oxide catalysts. *Appl. Catal. B Environ.* **2003**, *40*, 43–49. [[CrossRef](#)]
49. Li, X.; Dai, H.; Deng, J.; Liu, Y.; Xie, S.; Zhao, Z.; Wang, Y.; Guo, G.; Arandiyán, H. Au/3DOMLaCoO<sub>3</sub>: High performance catalysts for the oxidation of carbon monoxide and toluene. *Chem. Eng. J.* **2013**, *228*, 965–975. [[CrossRef](#)]
50. Barakat, T.; Idakiev, V.; Cousin, R.; Shao, G.-S.; Yuan, Z.-Y.; Tabakova, T.; Siffert, S. Total oxidation of toluene over noble metal based Ce, Fe and Ni doped titanium oxides. *Appl. Catal. B Environ.* **2014**, *146*, 138–146. [[CrossRef](#)]
51. Haruta, M.; Yamada, N.; Kobayashi, T.; Iijima, S. ChemInform Abstract: Gold Catalysts Prepared by Coprecipitation for Low-Temperature Oxidation of Hydrogen and of Carbon Monoxide. *J. Catal.* **1989**, *115*, 301–309. [[CrossRef](#)]

52. Scirè, S.; Liotta, L.F. Supported gold catalysts for the total oxidation of volatile organic compounds. *Appl. Catal. B. Environ.* **2012**, *125*, 222–246. [[CrossRef](#)]
53. Haruta, M.; Daté, M. Advances in the catalysis of Au nanoparticles. *Appl. Catal. A Gen.* **2001**, *222*, 427–437. [[CrossRef](#)]
54. Guan, Y.; Hensen, E.J. Ethanol dehydrogenation by gold catalysts: The effect of the gold particle size and the presence of oxygen. *Appl. Catal. A Gen.* **2009**, *361*, 49–56. [[CrossRef](#)]
55. Haruta, M. Size- and support-dependency in the catalysis of gold. *Catal. Today* **1997**, *36*, 153–166. [[CrossRef](#)]
56. Solsona, B.; Garcia, T.; Aylón, E.; Dejoz, A.M.; Vázquez, I.; Agouram, S.; Davies, T.E.; Taylor, S.H. Promoting the activity and selectivity of high surface area Ni-Ce-O mixed oxides by gold deposition for VOC catalytic combustion. *Chem. Eng. J.* **2011**, *175*, 271–278. [[CrossRef](#)]
57. Kim, K.-J.; Ahn, H.-G. Complete oxidation of toluene over bimetallic Pt–Au catalysts supported on ZnO/Al<sub>2</sub>O<sub>3</sub>. *Appl. Catal. B Environ.* **2009**, *91*, 308–318. [[CrossRef](#)]
58. Nevanperä, T.K.; Pitkääho, S.; Keiski, R.L. Oxidation of dichloromethane over Au, Pt, and Pt–Au containing catalysts supported on  $\gamma$ -Al<sub>2</sub>O<sub>3</sub> and CeO<sub>2</sub>-Al<sub>2</sub>O<sub>3</sub>. *Molecules* **2020**, *25*, 4644. [[CrossRef](#)] [[PubMed](#)]
59. Corma, A.; Garcia, H. Supported gold nanoparticles as catalysts for organic reactions. *Chem. Soc. Rev.* **2008**, *37*, 2096–2126. [[CrossRef](#)] [[PubMed](#)]
60. Santos, V.P.; Carabineiro, S.A.C.; Tavares, P.B.; Pereira, M.F.R.; Órfão, J.J.M.; Figueiredo, J.L. Oxidation of CO, ethanol and toluene over TiO<sub>2</sub> supported noble metal catalysts. *Appl. Catal. B* **2010**, *99*, 198–205. [[CrossRef](#)]
61. Gutiérrez, L.-F.; Hamoudi, S.; Belkacemi, K. Synthesis of Gold Catalysts Supported on Mesoporous Silica Materials: Recent Developments. *Catalysts* **2011**, *1*, 97–154. [[CrossRef](#)]
62. Gaálová, J.; Topka, P. Gold and Ceria as Catalysts for VOC Abatement: A Review. *Catalysts* **2021**, *11*, 789. [[CrossRef](#)]
63. Centeno, M.; Paulis, M.; Montes, M.; Odriozola, J.A. Catalytic combustion of volatile organic compounds on gold/titanium oxynitride catalysts. *Appl. Catal. B Environ.* **2005**, *61*, 177–183. [[CrossRef](#)]
64. Zhang, X.; Corma, A. Supported Gold(III) Catalysts for Highly Efficient Three-Component Coupling Reactions. *Angew. Chem.* **2008**, *120*, 4430–4433. [[CrossRef](#)]
65. Guisnet, M.; Dégé, P.; Magnoux, P. Catalytic oxidation of volatile organic compounds 1. Oxidation of xylene over a 0.2 wt% Pd/HFAU(17) catalyst. *Appl. Catal. B Environ.* **1999**, *20*, 1–13. [[CrossRef](#)]
66. Dégé, P.; Pinard, L.; Magnoux, P.; Guisnet, M. Catalytic oxidation of volatile organic compounds: II. Influence of the physicochemical characteristics of Pd/HFAU catalysts on the oxidation of o-xylene. *Appl. Catal. B* **2020**, *27*, 17–26. [[CrossRef](#)]
67. Liu, Z.-S.; Chen, J.-Y.; Peng, Y.-H. Activated carbon fibers impregnated with Pd and Pt catalysts for toluene removal. *J. Hazard. Mater.* **2013**, *256–257*, 49–55. [[CrossRef](#)]
68. Bi, F.; Zhang, X.; Chen, J.; Yang, Y.; Wang, Y. Excellent catalytic activity and water resistance of UiO-66-supported highly dispersed Pd nanoparticles for toluene catalytic oxidation. *Appl. Catal. B Environ.* **2020**, *269*, 118767. [[CrossRef](#)]
69. Gil, S.; Garcia-Vargas, J.M.; Liotta, L.F.; Pantaleo, G.; Ousmane, M.; Retailleau, L.; Giroir-Fendler, A. Catalytic Oxidation of Propene over Pd Catalysts Supported on CeO<sub>2</sub>, TiO<sub>2</sub>, Al<sub>2</sub>O<sub>3</sub> and M/Al<sub>2</sub>O<sub>3</sub> Oxides (M = Ce, Ti, Fe, Mn). *Catalysts* **2015**, *5*, 671–689. [[CrossRef](#)]
70. Weng, X.; Shi, B.; Liu, A.; Sun, J.; Xiong, Y.; Wan, H.; Zheng, S.; Dong, L.; Chen, Y.-W. Highly dispersed Pd/modified-Al<sub>2</sub>O<sub>3</sub> catalyst on complete oxidation of toluene: Role of basic sites and mechanism insight. *Appl. Surf. Sci.* **2019**, *497*, 143747. [[CrossRef](#)]
71. He, C.; Li, P.; Cheng, J.; Li, J.; Hao, Z. Preparation and investigation of Pd/Ti-SBA-15 catalysts for catalytic oxidation of benzene. *Environ. Prog. Sustain. Energy* **2010**, *29*, 435–442. [[CrossRef](#)]
72. He, C.; Li, J.; Li, P.; Cheng, J.; Hao, Z.; Xu, Z.P. Comprehensive investigation of Pd/ZSM-5/MCM-48 composite catalysts with enhanced activity and stability for benzene oxidation. *Appl. Catal. B* **2010**, *96*, 466–475. [[CrossRef](#)]
73. Li, P.; He, C.; Cheng, J.; Ma, C.Y.; Dou, B.J.; Hao, Z.P. Catalytic oxidation of toluene over Pd/Co<sub>3</sub>AlO catalysts derived from hydrotalcite-like compounds: Effects of preparation methods. *Appl. Catal. B Environ.* **2011**, *101*, 570–579. [[CrossRef](#)]
74. Zhao, S.; Hu, F.; Li, J. Hierarchical Core-Shell Al<sub>2</sub>O<sub>3</sub>@Pd-CoAlO Microspheres for Low-Temperature Toluene Combustion. *ACS Catal.* **2016**, *6*, 3433–3441. [[CrossRef](#)]
75. Wang, H.; Yang, W.; Tian, P.; Zhou, J.; Tang, R.; Wu, S. A highly active and anti-coking Pd-Pt/SiO<sub>2</sub> catalyst for catalytic combustion of toluene at low temperature. *Appl. Catal. A Gen.* **2017**, *529*, 60–67. [[CrossRef](#)]
76. Hu, C. Catalytic combustion kinetics of acetone and toluene over Cu<sub>0.13</sub>Ce<sub>0.87</sub>O<sub>y</sub> catalyst. *Chem. Eng. J.* **2011**, *168*, 1185–1192. [[CrossRef](#)]
77. Giraudon, J.-M.; Nguyen, T.B.; Leclercq, G.; Siffert, S.; Lamonier, J.-F.; Aboukais, A.; Vantomme, A.; Su, B.-L. Chlorobenzene total oxidation over palladium supported on ZrO<sub>2</sub>, TiO<sub>2</sub> nanostructured supports. *Catal. Today* **2008**, *137*, 379–384. [[CrossRef](#)]
78. Pérez-Cadenas, A.F.; Morales-Torres, S.; Kapteijn, F.; Maldonado-Hódar, F.J.; Carrasco-Marín, F.; Moreno-Castilla, C.; Moulijn, J.A. Carbon-based monolithic supports for palladium catalysts: The role of the porosity in the gas-phase total combustion of m-xylene. *Appl. Catal. B* **2008**, *77*, 272–277. [[CrossRef](#)]
79. Wang, Y.; Zhang, C.; Yu, Y.; Yue, R.; He, H. Ordered mesoporous and bulk Co<sub>3</sub>O<sub>4</sub> supported Pd catalysts for catalytic oxidation of o-xylene. *Catal. Today* **2015**, *242*, 294–299. [[CrossRef](#)]
80. Wei, Y.; Zhang, X.; Liu, Y.; Jia, C.; Yang, P. Ternary PtNiCu self-assembled nanocubes for plasmon-enhanced electrocatalytic hydrogen evolution and methanol oxidation reaction in visible light. *Electrochim. Acta* **2020**, *349*, 136366. [[CrossRef](#)]

81. Chen, T.; Rodionov, V.O. Controllable Catalysis with Nanoparticles: Bimetallic Alloy Systems and Surface Adsorbates. *ACS Catal.* **2016**, *6*, 4025–4033. [[CrossRef](#)]
82. Wu, Z.; Deng, J.; Xie, S.; Yang, H.; Zhao, X.; Zhang, K.; Lin, H.; Dai, H.; Guo, G. Mesoporous Cr<sub>2</sub>O<sub>3</sub>-supported Au-Pd nanoparticles: High-performance catalysts for the oxidation of toluene. *Microporous Mesoporous Mater.* **2016**, *224*, 311–322. [[CrossRef](#)]
83. Chen, Z.; Li, J.; Yang, P.; Cheng, Z.; Li, J.; Zuo, S. Ce-modified mesoporous  $\gamma$ -Al<sub>2</sub>O<sub>3</sub> supported Pd-Pt nanoparticle catalysts and their structure-function relationship in complete benzene oxidation. *Chem. Eng. J.* **2019**, *356*, 255–261. [[CrossRef](#)]
84. Taylor, M.N.; Zhou, W.; Garcia, T.; Solsona, B.; Carley, A.F.; Kiely, C.J.; Taylor, S.H. Synergy between tungsten and palladium supported on titania for the catalytic total oxidation of propane. *J. Catal.* **2012**, *285*, 103–114. [[CrossRef](#)]
85. Yang, K.; Liu, Y.; Deng, J.; Zhao, X.; Yang, J.; Han, Z.; Hou, Z.; Dai, H. Three-dimensionally ordered mesoporous iron oxide-supported single-atom platinum: Highly active catalysts for benzene combustion. *Appl. Catal. B* **2019**, *244*, 650–659. [[CrossRef](#)]
86. Beauchet, R.; Magnoux, P.; Mijoin, J. Catalytic oxidation of volatile organic compounds (VOCs) mixture (isopropanol/o-xylene) on zeolite catalysts. *Catal. Today* **2007**, *124*, 118–123. [[CrossRef](#)]
87. Joung, H.J.; Kim, J.H.; Oh, J.S.; You, D.W.; Park, H.O.; Jung, K.W. Catalytic oxidation of VOCs over CNT-supported platinum nanoparticles. *Appl. Surf. Sci.* **2014**, *290*, 267–273. [[CrossRef](#)]
88. Aksoylu, A.E.; Madalena, M.; Freitas, A.; Pereira, M.F.R.; Figueiredo, J.L. The effects of different activated carbon supports and support modifications on the properties of Pt/AC catalysts. *Carbon* **2001**, *39*, 175–185. [[CrossRef](#)]
89. Mao, M.; Lv, H.; Li, Y.; Yang, Y.; Zeng, M.; Li, N.; Zhao, X. Metal Support Interaction in Pt Nanoparticles Partially Confined in the Mesopores of Microsized Mesoporous CeO<sub>2</sub> for Highly Efficient Purification of Volatile Organic Compounds. *ACS Catal.* **2016**, *6*, 418–427. [[CrossRef](#)]
90. Abbasi, Z.; Haghighi, M.; Fatehifar, E.; Saedy, S. Synthesis and physicochemical characterizations of nanostructured Pt/Al<sub>2</sub>O<sub>3</sub>-CeO<sub>2</sub> catalysts for total oxidation of VOCs. *J. Hazard. Mater.* **2011**, *186*, 1445–1454. [[CrossRef](#)]
91. Pitkääho, S.; Nevanperä, T.; Matejova, L.; Ojala, S.; Keiski, R.L. Oxidation of dichloromethane over Pt, Pd, Rh, and V<sub>2</sub>O<sub>5</sub> catalysts supported on Al<sub>2</sub>O<sub>3</sub>, Al<sub>2</sub>O<sub>3</sub>-TiO<sub>2</sub> and Al<sub>2</sub>O<sub>3</sub>-CeO<sub>2</sub>. *Appl. Catal. B Environ.* **2013**, *138–139*, 33–42. [[CrossRef](#)]
92. Peng, R.; Sun, X.; Li, S.; Chen, L.; Fu, M.; Wu, J.; Ye, D. Shape effect of Pt/CeO<sub>2</sub> catalysts on the catalytic oxidation of toluene. *Chem. Eng. J.* **2016**, *306*, 1234–1246. [[CrossRef](#)]
93. Assal, Z.E.; Ojala, S.; Pitkääho, S.; Pirault-Roy, L.; Darif, B.; Comparot, J.-D.; Bensitel, M.; Keiski, R.L.; Brahmi, R. Comparative study on the support properties in the total oxidation of dichloromethane over Pt catalysts. *Chem. Eng. J.* **2017**, *313*, 1010–1022. [[CrossRef](#)]
94. Yang, Y.; Wang, G.; Fang, D.; Han, J.; Dang, F.; Yang, M. Study of the use of a Pd-Pt-based catalyst for the catalytic combustion of storage tank VOCs. *Int. J. Hydrog. Energy* **2020**, *45*, 22732–22743. [[CrossRef](#)]
95. Shuo, W.; Wangwang, F.; Bowei, W.; Yuyao, Z.; Ligong, C.; Xilong, Y.; Guoyi, B.; Yang, L. Rh<sub>1</sub>Cu<sub>3</sub>/ZSM-5 as an efficient bi-functional catalyst/adsorbent for VOCs abatement. *Catal. Letters* **2021**, in press.
96. Hosokawa, S.; Taniguchi, M.; Utani, K.; Kanai, H.; Imamura, S. Affinity order among noble metals and CeO<sub>2</sub>. *Appl. Catal. A Gen.* **2005**, *289*, 115–120. [[CrossRef](#)]
97. Liu, X.; Chen, L.; Zhu, T.; Ning, R. Catalytic oxidation of chlorobenzene over noble metals (Pd, Pt, Ru, Rh) and the distributions of polychlorinated by-products. *J. Hazard. Mater.* **2019**, *363*, 90–98. [[CrossRef](#)]
98. Song, S.; Zhang, S.; Zhang, X.; Verma, P.; Wen, M. Advances in Catalytic Oxidation of Volatile Organic Compounds over Pd-Supported Catalysts: Recent Trends and Challenges. *Front. Mater.* **2020**, *7*, 595667. [[CrossRef](#)]
99. Kim, H.J.; Kim, J.H.; Kim, J.H.; Kim, H.S.; Ryu, J.H.; Kang, S.H.; Lee, S.C. Catalytic Combustion Technology Trends for Removal of Volatile Organic Compounds (VOCs). *J. Energy Clim. Change* **2021**, *16*, 149–170.
100. Wang, J.; Liu, X.; Zeng, J.; Zhu, T. Catalytic oxidation of trichloroethylene over TiO<sub>2</sub> supported ruthenium catalysts. *Catal. Commun.* **2016**, *76*, 13–18. [[CrossRef](#)]
101. He, F.; Muliane, U.; Weon, S.; Choi, W. Substrate-specific mineralization and deactivation behaviors of TiO<sub>2</sub> as an air-cleaning photocatalyst. *Appl. Catal. B Environ.* **2020**, *275*, 119145. [[CrossRef](#)]
102. Wang, Y.; Chen, Y.; Zhang, L.; Wang, G.; Deng, W.; Guo, L. Total catalytic oxidation of chlorinated aromatics over bimetallic Pt-Ru supported on hierarchical HZSM-5 zeolite. *Microporous Mesoporous Mater.* **2020**, *308*, 110538. [[CrossRef](#)]
103. Aranzabal, A.; González-Marcos, J.A.; Ayastuy, J.L.; González-Velasco, J.R. Kinetics of Pd/alumina catalysed 1,2-dichloroethane gas-phase oxidation. *Chem. Eng. Sci.* **2006**, *61*, 3564–3576. [[CrossRef](#)]
104. Cen, W.; Liu, Y.; Wu, Z.; Liu, J.; Wang, H.; Weng, X. Cl Species Transformation on CeO<sub>2</sub>(111) Surface and Its Effects on CVOCs Catalytic Abatement: A First-Principles Investigation. *J. Phys. Chem. C* **2014**, *118*, 6758–6766. [[CrossRef](#)]
105. Zhao, H.; Han, W.; Dong, F.; Tang, Z. Highly-efficient catalytic combustion performance of 1,2-dichlorobenzene over meso-porous TiO<sub>2</sub>-SiO<sub>2</sub> supported CeMn oxides: The effect of acid sites and redox sites. *J. Ind. Eng. Chem.* **2018**, *64*, 194–205. [[CrossRef](#)]
106. Dai, Q.; Wu, J.; Deng, W.; Hu, J.; Wu, Q.; Guo, L.; Sun, W.; Zhan, W.; Wang, X. Comparative studies of P/CeO<sub>2</sub> and Ru/CeO<sub>2</sub> catalysts for catalytic combustion of dichloromethane: From effects of H<sub>2</sub>O to distribution of chlorinated by-products. *Appl. Catal. B* **2019**, *249*, 9–18. [[CrossRef](#)]
107. Kröcher, O.; Elsener, M. Hydrolysis and oxidation of gaseous HCN over heterogeneous catalysts. *Appl. Catal. B Environ.* **2009**, *92*, 75–89. [[CrossRef](#)]

108. Cao, S.; Fei, X.; Wen, Y.; Sun, Z.; Wang, H.; Wu, Z. Bimodal mesoporous TiO<sub>2</sub> supported Pt, Pd and Ru catalysts and their catalytic performance and deactivation mechanism for catalytic combustion of Dichloromethane (CH<sub>2</sub>Cl<sub>2</sub>). *Appl. Catal. A Gen.* **2018**, *550*, 20–27. [[CrossRef](#)]
109. Kamal, M.S.; Razzak, S.A.; Hossain, M.M. Catalytic oxidation of volatile organic compounds (VOCs)—A review. *Atmos. Environ.* **2016**, *140*, 117–134. [[CrossRef](#)]
110. Zhang, C.; Wang, C.; Hua, W.; Guo, Y.; Lu, G.; Gil, S.; Giroir-Fendler, A. Relationship between catalytic deactivation and physicochemical properties of LaMnO<sub>3</sub> perovskite catalyst during catalytic oxidation of vinyl chloride. *Appl. Catal. B Environ.* **2016**, *186*, 173–183. [[CrossRef](#)]
111. Gallastegi-Villa, M.; Aranzabal, A.; Romero-Sáez, M.; González-Marcos, J.A.; González-Velasco, J.R. Catalytic activity of regenerated catalyst after the oxidation of 1,2-dichloroethane and trichloroethylene. *Chem. Eng. J.* **2014**, *241*, 200–206. [[CrossRef](#)]
112. Keav, S.; Martin, A.; Barbier, J.J.; Duprez, D. Deactivation and reactivation of noble metal catalysts tested in the Catalytic Wet Air Oxidation of phenol. *Catal. Today* **2010**, *151*, 143–147. [[CrossRef](#)]
113. Ammendola, P.; Chirone, R.; Ruoppolo, G.; Russo, G. Regeneration of spent catalysts in oxy-combustion atmosphere. *Exp. Therm. Fluid Sci.* **2010**, *34*, 262–268. [[CrossRef](#)]
114. Kim, S.C.; Shim, W.G. Influence of physicochemical treatments on iron-based spent catalyst for catalytic oxidation of toluene. *J. Hazard. Mater.* **2008**, *154*, 310–316. [[CrossRef](#)] [[PubMed](#)]
115. Vu, V.H.; Belkouch, J.; Ould-Dris, A.; Taouk, B. Removal of hazardous chlorinated VOCs over Mn–Cu mixed oxide based catalyst. *J. Hazard. Mater.* **2009**, *169*, 758–765. [[CrossRef](#)] [[PubMed](#)]
116. Oliveira, L.C.A.; Lago, R.M.; Fabris, J.D.; Sapag, K. Catalytic oxidation of aromatic VOCs with Cr or Pd-impregnated Al-pillared bentonite: Byproduct formation and eactivation studies. *Appl. Clay. Sci.* **2008**, *39*, 218–222. [[CrossRef](#)]
117. Gallastegi-Villa, M.; Romero-Sáez, M.; Aranzabal, A.; Marcos, J.A.G.; González-Velasco, J.R. Strategies to enhance the stability of h-bea zeolite in the catalytic oxidation of Cl-VOCs: 1,2-Dichloroethane. *Catal. Today* **2013**, *213*, 192–197. [[CrossRef](#)]
118. Cuicui, D.; Shengyong, L.; Qiuling, W.; Alfons, G.B.; Mingjiang, N.; Damien, P.D. A review on catalytic oxidation of chloroaromatics from flue gas. *Chem. Eng. J.* **2018**, *334*, 419–544.
119. Sun, P.; Chen, J.; Zai, S.; Gao, S.; Weng, X.; Wu, Z. Regeneration mechanism of a deactivated zeolite-supported catalyst for the combustion of chlorinated volatile organic compounds. *Catal. Sci. Technol.* **2021**, *11*, 923–933. [[CrossRef](#)]